

Towards precise collider predictions: the Parton Branching method

Aleksandra Lelek

*Department of Physics, Particle Physics Group, Groenenborgerlaan 171,
2020 Antwerp, Belgium*

Contribution to the 19th International Conference on Hadron Spectroscopy and Structure (HADRON2021)

The collinear factorization theorem, combined with finite-order calculations in perturbative QCD, provides a powerful framework to obtain predictions for many collider observables. However, for observables which involve multiple energy scales, transverse degrees of freedom cannot be neglected, and finite-order perturbative calculations have to be combined with resummed calculations to all orders in the QCD running coupling in order to obtain reliable theoretical predictions, capable of describing experimental measurements. This is traditionally done either by analytic resummation methods or by parton shower (PS) Monte Carlo (MC) methods. In this talk we present the Parton Branching (PB) MC method to obtain QCD collider predictions based on Transverse Momentum Dependent (TMD) factorization. The PB provides evolution equations for TMD Parton Distribution Functions (PDFs) which, upon fitting TMD PDFs to experimental data, can be used in TMD MC event generators. We present the basic concepts of the method and illustrate its applications to collider measurements focusing on Drell-Yan (DY) lepton-pair production in different kinematic ranges, from fixed-target to LHC energies. We discuss the latest developments of the method concentrating especially on the matching of next-to-leading-order (NLO) TMD evolution with MC-at-NLO calculations of NLO matrix elements.

Keywords: Transverse Momentum Dependent (TMD) PDFs, resummation, Parton Shower, matching, NLO, Drell-Yan, Drell-Yan + jets, merging

1. Introduction

The collinear factorization theorem [1] is a baseline in obtaining QCD predictions for production processes at high energy colliders. Despite its indisputable success, for some observables involving more scales the transverse degrees of freedom of the proton have to be taken into account to obtain precise predictions [2]. The formalism to follow in such scenarios is the Transverse Momentum Dependent (TMD) factorization theorem which can take the form of analytical Collins-Soper-Sterman (CSS) approach [3] or high energy (k_{\perp}) factorization [4, 5]. In practical applications, the soft gluons resummation is performed by Parton Shower (PS) algorithms within Monte Carlo (MC) generators.

In recent years a MC method is being developed which makes use of TMD parton distribution functions (PDFs), commonly named as TMDs. The so called Parton Branching (PB) approach [6–8] turned out to be very flexible and enabled to perform studies in multiple directions [9–20]. In this work we concentrate on the successful description of Drell-Yan (DY) and DY + jets data in a wide kinematic range.

The precision measurements at high energy colliders rely up to a large extent on our understanding of the DY processes. As a clean production channel, DY is used in precision electro-weak measurements. DY data are used to extract

parton distribution functions (PDFs) and at low masses and low energies give access to study partons' intrinsic transverse momentum. DY is crucial for our understanding of QCD evolution and soft gluons resummation. DY + jets is of particular interest since the production channels important for precision measurements and beyond the standard model (BSM) searches involve final states with large multiplicities of jets. DY+jets is an important background in many measurements. It is also used in studies on multiparton interactions.

The theoretical description of DY p_{\perp} spectra over wide kinematic regions in energy, mass and p_{\perp} requires a proper matching between the fixed-order perturbative QCD calculations in the high p_{\perp} region (i.e. $p_{\perp} \gtrsim Q$, where Q is the invariant mass of the DY lepton pair) and soft gluon resummation in the low p_{\perp} region ($p_{\perp} \ll Q$).

Recent studies [21] showed that the perturbative fixed-order calculations in collinear factorization are not able to describe the DY p_T spectra for $p_{\perp} \sim Q$ at fixed target experiments. In sec. 3. we investigate this issue from the standpoint of the PB approach.

The possible impact of TMDs on multi-jet production has just started to be explored. In sec. 4. this topic is addressed, and the new PB result for merged DY+jets calculation including higher jets multiplicities is discussed [19].

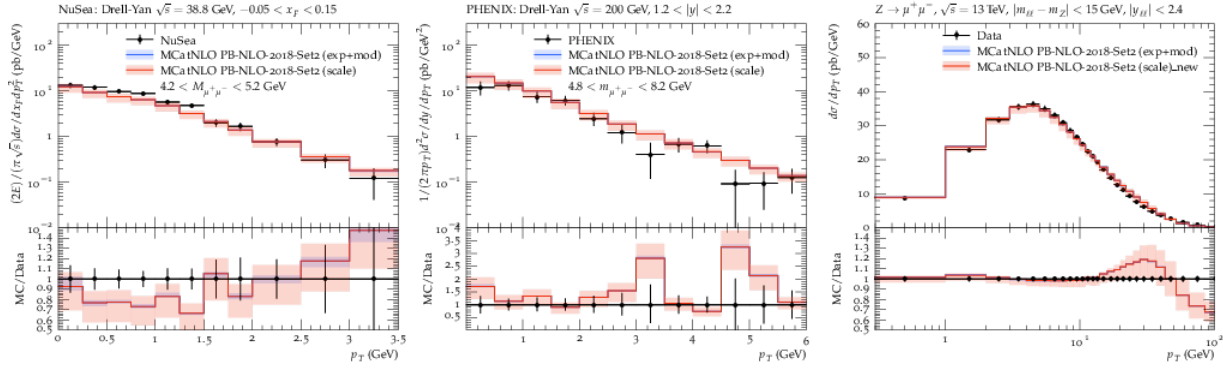


Figure 1: Predictions for DY p_{\perp} spectra obtained with MCatNLO+PB TMD compared with data coming from NuSea (left), PHENIX (middle) and CMS (right) experiments [14].

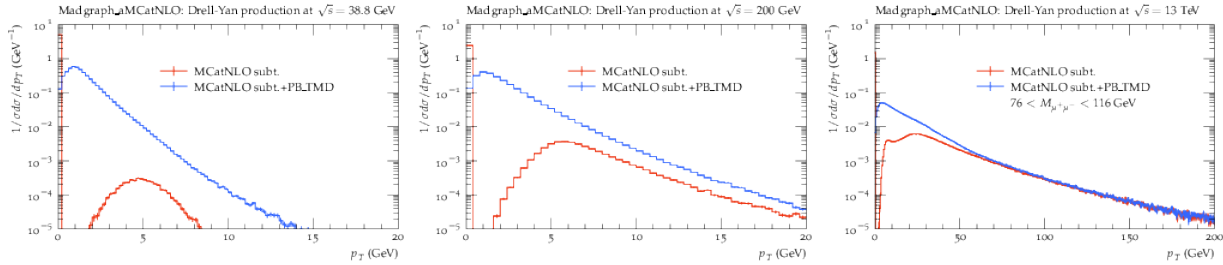


Figure 2: Subtracted NLO ME from MCatNLO calculation (red) and full MCatNLO+PB TMD calculation (blue) at center of mass energies corresponding to Fig. 1 [14].

2. The Parton Branching method

In the PB method the TMDs are obtained from the PB TMD evolution equation [6, 7]. The equation is based on showering [22] version of the DGLAP equation [23–26] where the unitarity picture is used: parton evolution is expressed in terms of real, resolvable branching probabilities, provided by the real emission DGLAP splitting functions and no-branching probabilities, included via Sudakov form factors. The equation describes the change of the TMD $\tilde{A}_a(x, k_{\perp}, \mu) = xA_a(x, k_{\perp}, \mu)$ for all flavors a with the evolution scale μ calculating the longitudinal fraction x of the protons' momentum and the transverse momentum k_{\perp} carried by the parton after each branching. The starting distribution at initial evolution scale includes the longitudinal momentum part and the intrinsic transverse momentum $k_{\perp 0}$. Using a parameterization of the HERAPDF2.0 [27] form for the longitudinal momentum and a Gaussian in $k_{\perp 0}$, the parameters of the longitudinal part are fitted [8] to the HERA DIS data using xFitter [28]. The transverse momentum is accumulated at each branching: it is a sum of the intrinsic transverse momentum and all the transverse momenta q_{\perp} emitted in the evolution chain. The branchings in the PB method are angular ordered (AO) [7, 12] which allows to perform soft gluons resummation. The AO enters the PB method similarly to [22], i.e. via 3 elements: 1. relating the DGLAP evolution scale μ to branching variables z (which is the ratio of the x variables of the partons propagating towards the hard scattering before and after the branching) and q_{\perp} , 2. in the

scale of running coupling $\alpha_s(q_{\perp})$ and 3. in the definition of the soft gluons resolution scale z_M , which is the maximum value allowed for z variable for a parton to be considered resolvable.

Delivered PB TMDs can be accessed via TMDlib [29] and used in TMD MC generators (like e.g. CASCADE [30, 31]). Additionally, the PB TMDs can be integrated over k_{\perp} to obtain collinear PDFs $x f(x, \mu)$ (or so called integrated TMDs, iTMDs) which can be then used via LHAPDF [32] in collinear physics applications and tools. The PB parton distributions are applicable in a wide kinematic range of x , k_{\perp} and μ .

3. DY predictions with the PB method

The technique to obtain collider predictions with PB TMDs was proposed in [8]. In [13] the method was further developed to next-to-leading (NLO) where PB TMDs were combined with NLO matrix element (ME) within the MADGRAPH5_AMC@NLO (referred later as MCatNLO) [33].

The first step of the generation is performed by MCatNLO. The so called subtracted collinear NLO ME is generated in the LHE format [34] using the integrated PB TMD via LHAPDF. In order to avoid possible double counting when combining NLO ME with PS, the MCatNLO method uses subtraction terms for soft and collinear contributions [35]. In the procedure presented here PB TMDs

are used instead of PS, their role is however very similar. Because of that the subtraction method has to be used to combine PB TMDs with MCatNLO calculations. The exact form of the subtraction terms depends on the PS algorithm. The AO used in PB TMDs is similar to Herwig6 [36] so MCatNLO with Herwig6 subtraction is used to combine PB TMDs with MCatNLO. In the next step the subtracted collinear ME is supplemented with transverse momentum k_\perp by an algorithm in CASCADE, and k_\perp is added to the event record according to the TMD distribution. The TMD used in CASCADE corresponds to the iTMD from which the ME was initially generated. The longitudinal momentum fractions of the incoming partons have to be adjusted to conserve energy-momentum and keep the mass of the DY system unchanged. For inclusive observables, like DY p_\perp spectrum, the whole kinematics is included by using PB TMDs.

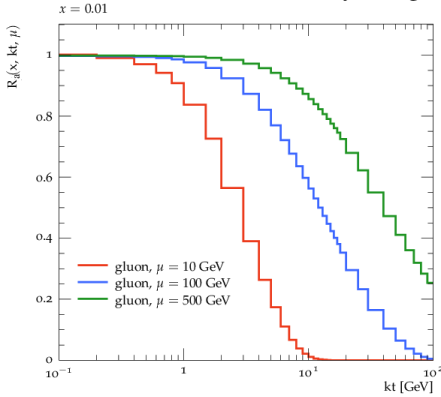


Figure 3: The k_\perp dependence of the ratio defined in eq. 1 calculated for gluon at $x = 0.01$ at different evolution scales μ [19].

The described procedure using PB-NLO-HERAI+II-2018-set2 TMD PDF [8] was applied to obtain predictions for DY p_\perp data from different experiments at very different center of mass energies \sqrt{s} and DY masses [14]: NuSea [37], R209 [38], PHENIX [39], ATLAS [42] and CMS [41]. The results for spectra coming from NuSea, PHENIX and CMS are presented in fig. 1 showing a good description in all these kinematic regimes in small and middle p_\perp range. To obtain a proper prediction in the high p_\perp range, higher jet multiplicities have to be taken into account. This will be discussed in the next section.

In Fig. 2 the MCatNLO+PB TMD prediction (blue) is compared to MCatNLO subtracted ME calculation (red) for center of mass energies corresponding to measurements presented in Fig. 1. At low DY mass and low energy, the contribution of soft gluon emissions contained in PB TMDs is crucial to describe the data even in the region of $p_\perp \sim Q$. The situation is different at LHC energies and larger masses, where the contribution from soft gluons in the region of $p_\perp \sim Q$ is small and the spectrum is governed by hard real emission. This confirms the observation from the literature that perturbative fixed-order calculations in collinear factorization are not able to describe DY p_\perp spectra at fixed target

experiments in the region of $p_\perp \sim Q$.

4. TMD effects at high p_\perp

It is commonly known that TMD effects play a role at scales of order of few GeV. The question remains if they can be also important at higher scales. In the PB approach the TMD at the initial evolution scale $\mu \sim \mathcal{O}(1 \text{ GeV})$ is a Gaussian with width σ , $\Lambda_{QCD} < \sigma < \mathcal{O}(1 \text{ GeV})$. During the evolution the transverse momentum k_\perp is accumulated in each step which leads to TMD broadening. In the PB method, the PDFs can be obtained from a TMD by integration over the transverse momentum $\tilde{f}_a(x, \mu^2) = \int dk_\perp^2 \tilde{A}_a(x, k_\perp, \mu^2)$. In order to estimate what is the probability of a parton a with momentum fraction x to acquire the transverse momentum higher than k_\perp at a given evolution scale μ one can define a ratio [19]

$$R_a(x, k_\perp, \mu^2) = \frac{\int_{k_\perp^2}^{\infty} dk_\perp'^2 \tilde{A}_a(x, k_\perp', \mu^2)}{\int dk_\perp'^2 \tilde{A}_a(x, k_\perp', \mu^2)} \quad (1)$$

which is shown in fig. 3 for 3 different evolution scales for gluon at $x = 0.01$. From this figure one can estimate e.g. that at $\mu = 100 \text{ GeV}$ the probability of a gluon to have a transverse momentum higher than 20 GeV is 30%. In other words, at LHC the contribution from the k_\perp -broadening of the TMD to e.g. the emission of an extra jet in a process characterized by a hard scale μ being the transverse momentum of a jet is comparable to emissions from hard matrix element [19].

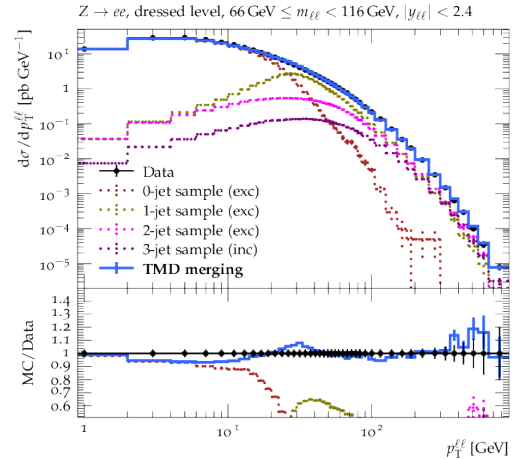


Figure 4: The fully TMD-merged calculation, as well as separate contributions from the different jet samples compared to 8 TeV ATLAS data for DY p_\perp spectrum [19].

It was shown in [13] that the proper description of the high p_\perp part of the DY spectrum requires the contribution from higher jet multiplicities. In [19] the standard MLM merging procedure [43, 44] was extended to the TMD case at leading order (LO). The TMD merging was applied to Z boson production in association with jets. Predictions coming from contributions from different jet samples and fully merged calculation

is compared to 8 TeV ATLAS data [42] in fig. 4. The merged calculation gives a good description of the data in the whole p_{\perp} range of the DY spectrum. One can see that at low p_{\perp} Z+0 jet sample is the main contribution to the spectrum and the importance of the higher multiplicities increases with p_{\perp} . In fig. 5 the predictions for jet multiplicity in Z+jets production obtained with merged calculation as well separate contributions from each jet multiplicity sample is compared with 13 TeV ATLAS data [45]. The agreement with data is excellent, also for the jet multiplicities higher than the maximum number of jets generated at the ME level.

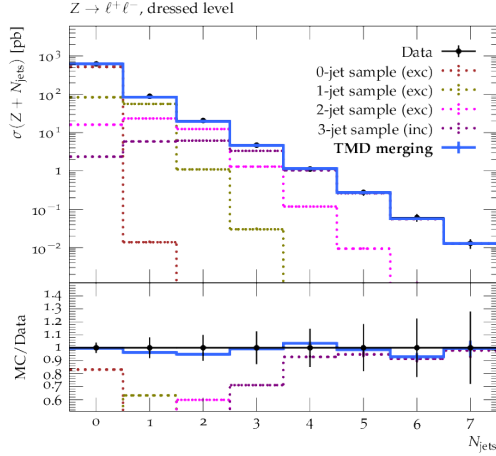


Figure 5: The fully TMD-merged calculation, as well as separate contributions from the different jet samples compared to 13 TeV ATLAS data for jet multiplicity in Z+jets production [19].

5. Conclusions

A central part of the LHC physics program are the precision strong and electro-weak measurements. For these, the accu-

racy of theoretical predictions of DY and DY+jets data is very important.

In this work the predictions obtained from the PB method for the DY p_{\perp} measurements over a wide range in energy, DY mass and p_{\perp} are shown. At low mass and low energy both fixed-order QCD and all-order soft gluon emissions are important to describe the DY p_{\perp} , and the reliability of the theoretical predictions depends on matching between those two elements. In the presented method in low and middle p_{\perp} range the NLO ME was combined with PB TMDs with the matching performed according to MCatNLO method. This allowed one to confirm the observation from the literature that perturbative fixed-order calculations in collinear factorization are not able to describe DY p_{\perp} spectra at fixed target experiments in the region of $p_{\perp} \sim Q$. Moreover it was noticed that the contribution from soft gluons included in PB TMDs is essential to describe these data. The situation changes with the center of mass energy: at LHC the region of $p_{\perp} \sim Q$ is well described by the collinear NLO calculation.

It was shown that because of the TMD broadening, the TMD effects cannot be neglected at high p_{\perp} . The high p_{\perp} region of the DY spectrum requires taking into account contributions from higher orders. The new TMD merging method was recently developed at LO to merge different jet multiplicities. With this method a very good description of the LHC DY p_{\perp} spectrum in the whole p_{\perp} region was obtained. The study opens the possibility to further investigate TMD effects at the level of exclusive jet observables and in the region of the highest p_{\perp} , where e.g. signals of BSM physics could be largest.

Acknowledgments

I acknowledge funding by Research Foundation-Flanders (FWO) (application number: 1272421N).

1. J. C. Collins, D. E. Soper, G. F. Sterman, Adv. Ser. Direct. High Energy Phys. **5** (1989)1 doi:10.1142/9789814503266-0001 [hep-ph/0409313].
2. R. Angeles-Martinez *et al.*, Acta Phys. Polon. B **46** (2015) no.12, 2501 doi:10.5506/APhysPolB.46.2501 [arXiv:1507.05267 [hep-ph]].
3. J. C. Collins, D. E. Soper, G. F. Sterman, Nucl. Phys. B **250** (1985) 199doi:10.1016/0550-3213(85)90479-1
4. S. Catani, M. Ciafaloni, F. Hautmann, Phys. Lett. B **242** (1990) 97doi:10.1016/0370-2693(90)91601-7
5. S. Catani, M. Ciafaloni, F. Hautmann, Nucl. Phys. B **366** (1991) 135doi:10.1016/0550-3213(91)90055-3
6. F. Hautmann, H. Jung, A. Lelek, V. Radescu, R. Zlebčik, Phys. Lett. B **772** (2017) 446 doi:10.1016/j.physletb.2017.07.005 [arXiv:1704.01757 [hep-ph]].
7. F. Hautmann, H. Jung, A. Lelek, V. Radescu, R. Zlebčik, JHEP **1801** (2018) 070 doi:10.1007/JHEP01(2018)070 [arXiv:1708.03279 [hep-ph]].
8. A. Bermudez Martinez, P. Connor, H. Jung, A. Lelek, R. Žlebčik, F. Hautmann and V. Radescu, Phys. Rev. D **99** (2019) no.7, 074008 doi:10.1103/PhysRevD.99.074008 [arXiv:1804.11152 [hep-ph]].
9. M. Deak, A. van Hameren, H. Jung, A. Kusina, K. Kutak and M. Serino, Phys. Rev. D **99** (2019) no.9, 094011 doi:10.1103/PhysRevD.99.094011 [arXiv:1809.03854 [hep-ph]].
10. E. Blanco, A. van Hameren, H. Jung, A. Kusina and K. Kutak, Phys. Rev. D **100** (2019) no.5, 054023 doi:10.1103/PhysRevD.100.054023 [arXiv:1905.07331 [hep-ph]].

11. H. Van Haevermaet, A. Van Hameren, P. Kotko, K. Kutak and P. Van Mechelen, *Eur. Phys. J. C* **80** (2020) no.7, 610 doi:10.1140/epjc/s10052-020-8193-2 [arXiv:2004.07551 [hep-ph]].
12. F. Hautmann, L. Keersmaekers, A. Lelek, A. M. Van Kampen, *Nucl. Phys. B* **949** (2019), 114795 doi:10.1016/j.nuclphysb.2019.114795 [arXiv:1908.08524 [hep-ph]].
13. A. Bermudez Martinez, P. Connor, D. Dominguez Damiani, L. I. Estevez Banos, F. Hautmann, H. Jung, J. Lidrych, M. Schmitz, S. Taheri Monfared and Q. Wang, *et al. Phys. Rev. D* **100** (2019) no.7, 074027 doi:10.1103/PhysRevD.100.074027 [arXiv:1906.00919 [hep-ph]].
14. A. Bermudez Martinez, P. L. S. Connor, D. Dominguez Damiani, L. I. Estevez Banos, F. Hautmann, H. Jung, J. Lidrych, A. Lelek, M. Mendizabal and M. Schmitz, *et al. Eur. Phys. J. C* **80** (2020) no.7, 598 doi:10.1140/epjc/s10052-020-8136-y [arXiv:2001.06488 [hep-ph]].
15. H. Jung, S. T. Monfared and T. Wening, [arXiv:2106.07010 [hep-ph]].
16. S. Taheri Monfared, H. Jung and F. Hautmann, *PoS ICHEP2020* (2021), 511 doi:10.22323/1.390.0511
17. L. Keersmaekers and S. T. Monfared, [arXiv:2111.02113 [hep-ph]].
18. L. Keersmaekers, [arXiv:2109.07326 [hep-ph]].
19. A. B. Martinez, F. Hautmann and M. L. Mangano, *Phys. Lett. B* **822**, 136700 (2021) doi:10.1016/j.physletb.2021.136700 [arXiv:2107.01224 [hep-ph]].
20. M. I. Abdulhamid, M. A. Al-Mashad, A. B. Martinez, G. Bonomelli, I. Bujanja, N. Crnkovic, F. Colombina, B. D'Anzi, S. Cerci and M. Davydov, *et al. Eur. Phys. J. C* **82**, no.1, 36 (2022) doi:10.1140/epjc/s10052-022-09997-1 [arXiv:2112.10465 [hep-ph]].
21. A. Bacchetta, G. Bozzi, M. Lambertsen, F. Piacenza, J. Steiglechner and W. Vogelsang, *Phys. Rev. D* **100**, no.1, 014018 (2019) doi:10.1103/PhysRevD.100.014018 [arXiv:1901.06916 [hep-ph]].
22. G. Marchesini, B. R. Webber, *Nucl. Phys. B* **310** (1988) 461 doi:10.1016/0550-3213(88)90089-2
23. V. N. Gribov, L. N. Lipatov, *Sov. J. Nucl. Phys.* **15** (1972) 438 [*Yad. Fiz.* **15** (1972) 781]
24. L. N. Lipatov, *Sov. J. Nucl. Phys.* **20** (1975) 94 [*Yad. Fiz.* **20** (1974) 181]
25. G. Altarelli, G. Parisi, *Nucl. Phys. B* **126** (1977) 298 doi:10.1016/0550-3213(77)90384-4
26. Y. L. Dokshitzer, *Sov. Phys. JETP* **46** (1977) 641 [*Zh. Eksp. Teor. Fiz.* **73** (1977) 1216]
27. H. Abramowicz *et al.* [H1 and ZEUS], *Eur. Phys. J. C* **75** (2015) no.12, 580 doi:10.1140/epjc/s10052-015-3710-4 [arXiv:1506.06042 [hep-ex]].
28. S. Alekhin *et al.*, *Eur. Phys. J. C* **75** (2015) 304 doi:10.1140/epjc/s10052-015-3480-z [arXiv:1410.4412 [hep-ph]].
29. N. A. Abdulov, A. Bacchetta, S. Baranov, A. B. Martinez, V. Bertone, C. Bissolotti, V. Candilise, L. I. E. Banos, M. Bury and P. L. S. Connor, *et al. Eur. Phys. J. C* **81** (2021), 752 doi:10.1140/epjc/s10052-021-09508-8 [arXiv:2103.09741 [hep-ph]].
30. H. Jung *et al.*, *Eur. Phys. J. C* **70** (2010) 1237 doi:10.1140/epjc/s10052-010-1507-z [arXiv:1008.0152 [hep-ph]].
31. S. Baranov, A. Bermudez Martinez, L. I. Estevez Banos, F. Guzman, F. Hautmann, H. Jung, A. Lelek, J. Lidrych, A. Lipatov and M. Malyshev, *et al. Eur. Phys. J. C* **81** (2021) no.5, 425 doi:10.1140/epjc/s10052-021-09203-8 [arXiv:2101.10221 [hep-ph]].
32. A. Buckley, J. Ferrando, S. Lloyd, K. Nordström, B. Page, M. Rüfenacht, M. Schönherr and G. Watt, *Eur. Phys. J. C* **75** (2015), 132 doi:10.1140/epjc/s10052-015-3318-8 [arXiv:1412.7420 [hep-ph]].
33. J. Alwall, R. Frederix, S. Frixione, V. Hirschi, F. Maltoni, O. Mattelaer, H. S. Shao, T. Stelzer, P. Torrielli, M. Zaro, *JHEP* **07** (2014), 079 doi:10.1007/JHEP07(2014)079 [arXiv:1405.0301 [hep-ph]].
34. J. Alwall, A. Ballestrero, P. Bartalini, S. Belov, E. Boos, A. Buckley, J. M. Butterworth, L. Dudko, S. Frixione and L. Garren, *et al. Comput. Phys. Commun.* **176** (2007), 300-304 doi:10.1016/j.cpc.2006.11.010 [arXiv:hep-ph/0609017 [hep-ph]].
35. S. Frixione and B. R. Webber, *JHEP* **06** (2002), 029 doi:10.1088/1126-6708/2002/06/029 [arXiv:hep-ph/0204244 [hep-ph]].
36. G. Corcella, I. G. Knowles, G. Marchesini, S. Moretti, K. Odagiri, P. Richardson, M. H. Seymour, B. R. Webber, [arXiv:hep-ph/0210213 [hep-ph]].
37. J. C. Webb, doi:10.2172/1155678 [arXiv:hep-ex/0301031 [hep-ex]].
38. D. Antreasyan, U. Becker, G. Bellettini, P. L. Braccini, J. G. Branson, J. D. Burger, F. Carbonara, R. Carrara, R. Castaldi, V. Cavasinni, *et al. Phys. Rev. Lett.* **48** (1982), 302 doi:10.1103/PhysRevLett.48.302
39. C. Aidala *et al.* [PHENIX], *Phys. Rev. D* **99** (2019) no.7, 072003 doi:10.1103/PhysRevD.99.072003 [arXiv:1805.02448 [hep-ex]].
40. G. Aad *et al.* [ATLAS], *Eur. Phys. J. C* **76** (2016) no.5, 291 doi:10.1140/epjc/s10052-016-4070-4 [arXiv:1512.02192 [hep-ex]].
41. A. M. Sirunyan *et al.* [CMS], *JHEP* **12** (2019), 061 doi:10.1007/JHEP12(2019)061 [arXiv:1909.04133 [hep-ex]].
42. G. Aad *et al.* [ATLAS], *Eur. Phys. J. C* **76** (2016) no.5, 291 doi:10.1140/epjc/s10052-016-4070-4 [arXiv:1512.02192 [hep-ex]].
43. M. L. Mangano, M. Moretti, F. Piccinini and M. Treccani, *JHEP* **01** (2007), 013 doi:10.1088/1126-6708/2007/01/013 [arXiv:hep-ph/0611129 [hep-ph]].
44. J. Alwall, S. Hoche, F. Krauss, N. Lavesson, L. Lonnblad, F. Maltoni, M. L. Mangano, M. Moretti, C. G. Papadopoulos and F. Piccinini, *et al. Eur. Phys. J. C* **53** (2008), 473-500 doi:10.1140/epjc/s10052-007-0490-5 [arXiv:0706.2569 [hep-ph]].
45. M. Aaboud *et al.* [ATLAS], *Eur. Phys. J. C* **77** (2017) no.6, 361 doi:10.1140/epjc/s10052-017-4900-z [arXiv:1702.05725 [hep-ex]].